Part-per-trillion trace selective gas detection using frequency locked whispering gallery mode microtoroids

Cheng Li[1], Trevor D. Lohrey[2], Phuong-Diem Nguyen[3], Zhouyang Min[3], Yisha Tang[3], Chang Ge[1], Zachary P. Sercel[2], Euan McLeod[1], Brian M. Stoltz[2] and Judith Su[1,3*]

[1]Wyant College of Optical Sciences, The University of Arizona, 1630 E University Blvd, Tucson, AZ 85721, USA
[2]The Warren and Katherine Schlinger Laboratory for Chemistry and Chemical Engineering, Division of Chemistry and Chemical Engineering, California Institute of Technology, Pasadena, CA 91125, USA
[3]Department of Biomedical Engineering, The University of Arizona, 1630 E University Blvd, Tucson, AZ 85721, USA

*judy@optics.arizona.edu

ABSTRACT:
Rapid detection of toxic and hazardous gases at trace concentrations plays a vital role in industrial, battlefield, and laboratory scenarios. Of interest are both sensitive as well as highly selective sensors. Whispering gallery mode (WGM) microresonator-based biochemical sensors are among the most sensitive sensors in existence due to their long photon confinement times. One main concern with these devices, however, is their selectivity towards specific classes of target analytes. Here, we employ frequency locked whispering gallery mode microtoroid optical resonators covalently modified with various polymer coatings to selectively detect the chemical warfare agent surrogate diisopropyl methylphosphonate (DIMP) as well as the toxic industrial chemicals formaldehyde and ammonia at parts-per-trillion concentrations. This is 1-2 orders of magnitude better than previously reported, depending on the target, except for pristine graphene and pristine carbon nanotube sensors, which demonstrate similar detection levels but in vacuum and without selectivity. Selective polymer coatings include polyethylene glycol (PEG) for DIMP sensing, accessed by the modification of commercially available materials, and 3-(triethoxysilyl)propyl-terminated polyvinyl acetate (PVAc) for ammonia sensing. Notably, we developed an efficient one-pot procedure to access 3-(triethoxysilyl)propyl-terminated PVAc that utilizes cobalt-mediated living radical polymerization and a nitroxyl polymer-terminating agent. Alkaline hydrolysis of PVAc coatings to form polyvinyl alcohol (PVA) coatings directly bound to the microtoroid proved to be reliable and reproducible, leading to WGM sensors capable of the rapid and selective detection of formaldehyde vapors. The selectivity of these three polymer coatings as sensing media was predicted, in part, based on their functional group content and known reactivity patterns with the target analytes. Furthermore, we demonstrate that microtoroids coated with a mixture of polymers can serve as an all-in-one sensor that can detect multiple agents. We anticipate that our results will facilitate rapid early detection of chemical agents, as well as their surrogates and precursors.

INTRODUCTION

Toxic and hazardous gases pose a threat to human health in industry, on the battlefield, and in laboratories. These gases are often colorless and odorless at low, but still harmful, concentrations, making their detection challenging. Accurate and rapid low concentration detection of these agents and their precursors can provide an early warning. Several gas sensing technologies and concepts emerged[1–5], all with different advantages and disadvantages in terms of their sensitivity, selectivity, stability, ease of preparation, expense, and portability. In particular, sensors based on pristine graphene and carbon nanotubes have demonstrated ultra-low limits of detection (sub-ppt) in response to nitric oxide, but lack selectivity to other gases and exhibit significant lab-to-lab variations in sensitivity[6,7]. Whispering gallery mode (WGM) microresonators stand apart from the rest of these biochemical sensors due to their long (on the order of nanoseconds) photon confinement times,[8–14] which causes increased interaction of light with matter and enables these devices to be ultra-sensitive sensors.[15,16] Here, we use a system previously developed in our lab known as FLOWER (frequency locked optical whispering evanescent resonator), which combines WGM technology with noise reduction techniques for sensitive detection of diisopropyl methylphosphonate (DIMP), ammonia (NH_3), and formaldehyde (CH_2O)[8,9,11]. We expand the selectivity of this technique using custom synthesized polymer coatings thus creating both an ultra-sensitive as well as selective on-chip sensor.

In this paper we outline the working principle of FLOWER and then describe the chemical syntheses of siloxy-terminated polymer films and the microtoroid coating method, followed by a detailed account of three different polymer-coated microtoroids containing polyethylene glycol (PEG), polyvinyl acetate (PVAc), and polyvinyl alcohol (PVA), to achieve the selective sensing of DIMP, ammonia, and formaldehyde vapors. Crucially, we find that PEG, PVAc, and PVA coatings each provide high sensitivity and selectivity for only one of the three target analytes. The limits of detection for each of these selective WGM sensors is in the parts per trillion regime. We also evaluate the stability of these polymer-coated toroids as a function of their sensing ability over time

(Figure S1). Finally, microcavity resonators coated with a mixture of PEG and PVAc lead to sensitivity and selectivity measurements consistent with those of the separate polymers, demonstrating the detection of multiple target analytes by a single WGM sensor.

FLOWER and gas vapor detection mechanism

In FLOWER, trace signals are detected by locking the frequency of the laser to the resonance frequency of the microresonator cavity (Figure 1a). The resonance condition of the microcavity is given by[10,17]:

$$m\lambda = n_{eff} \cdot 2\pi R, \qquad (\mathbf{1})$$

where m is the azimuthal mode number, n_{eff} is the effective refractive index of the WGM, and R is the principal radius of the microcavity. As molecules enter the evanescent field of the resonator, the resonance frequency of the cavity shifts. The laser frequency shifts accordingly and is used to measure the change in resonance frequency of the cavity. Light is evanescently coupled into the microcavity resonator using a tapered optical fiber and quasi totally internally reflects around the rim. The transmitted signal through the optical fiber is received by an auto-balanced photoreceiver and multiplied by a dither signal to generate an error signal that is the difference between the laser frequency and the microcavity resonance frequency

For these experiments, we use microtoroid optical resonators due to their high quality (Q) factors and on-chip fabrication. High Q enables precision tracking of the resonance. It is defined as $Q = \frac{\lambda_{Res}}{\lambda_{FWHM}}$, which is the ratio of the resonant wavelength to the linewidth. The Q of the uncoated toroid is typically $10^6 - 10^8$. Chemical coatings can introduce scattering losses and thus lower the Q factor. However, in our study, a uniform thin film polymer coating on the surface of the toroid enables a post-coating Q $> 5 \times 10^5$.

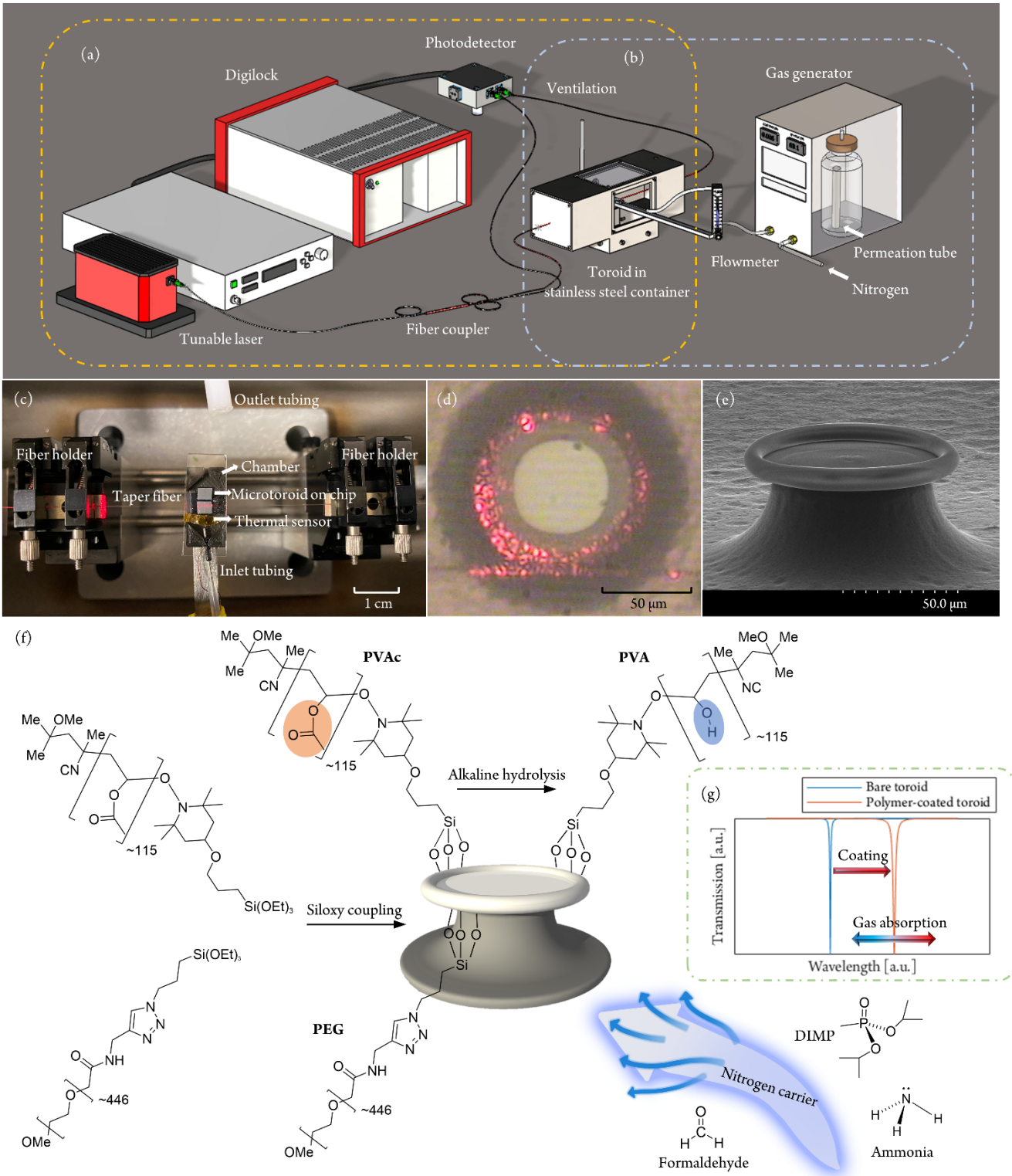

Figure 1. FLOWER gas detection system (not to scale). (a) In FLOWER, light from a tunable laser (in this case centered at 636 nm) is frequency locked to the cavity resonance for high precision tracking of the toroid resonance as molecules enter its evanescent field. (b) For gas sensing purposes, the toroid is enclosed in a vented stainless-steel chamber. Desired chemicals of interest are heated and directed into the chamber at a known concentration (c) Photograph of toroids mounted on sample stage. A commercial temperature probe is placed near the inlet tubing to monitor airflow temperature changes. (d) Top view of an optical fiber evanescently coupled to a microtoroid resonator. (e) Scanning electron micrograph of a microtoroid. The toroids used in these experiments are ~ 80 microns in diameter. (f) Schematic diagram of microtoroid gas sensor and gas detection process. The polymer layer is coated on the toroid surface using siloxy coupling chemistry and reacts selectively with the low concentration of target gas carried by the nitrogen. The orange and blue shaded ovals highlight the difference between PVAc and PVA. (g) Sensing mechanism of the wavelength shift induced by the coating and chemical reaction corresponding to the processes shown in (f). Ultra-thin polymer coatings still introduce slight radius changes that cause a shift to longer wavelengths (red shifts), and the associated scattering losses broaden the resonance The signal change due to the absorbed gas is determined by both a in change in radius of the microcavity and a change in refractive index.

As the target gas diffuses into the polymer coating, the refractive index change and the polymer swelling contribute to a change in cavity resonance conditions, as shown in Figure 1(g), which can be expressed as[18–20]:

$$\frac{\Delta\lambda}{\lambda} = \frac{\Delta n}{n} + \frac{\Delta R}{R}, \quad (\mathbf{2})$$

where R is the major radius of the toroid, n is the refractive index of the polymer-toroid system, and λ is the resonance frequency of the toroid. The interaction of gas vapors with a polymer may lead to sorption, which involves accumulation of the analyte on or within the polymer coating, or chemical reactions that directly modify the structure of the polymer. These two distinct processes are likely to have varying impacts on the resonance wavelength of the FLOWER gas sensor by affecting both the effective refractive index and principal radius of the system. In the course of designing a FLOWER gas sensor, we posited that well-known chemical reactions could provide a basis for the selective detection of low concentrations of gas vapors, wherein the functional groups of a polymer coating are chemically modified by the analyte(s) of interest, leading to a distinct change in refractive index.

We identified two distinct, well-established chemical reactions that could potentially allow for the sensitive and selective detection of specific trace gas vapors, namely the irreversible deacetylation of esters by ammonia and the reversible 1,2-addition of alcohols to formaldehyde.[21–24] These reactions, as depicted in Figure 2, inspired our evaluation of polyvinyl acetate (PVAc) and polyvinyl alcohol (PVA) as coatings in WGM gas sensing devices. Notably PVAc has previously been employed as a sorbent medium in ammonia gas sensing devices (LOD = 23 ppm),[25] and PVA has been utilized in films for formaldehyde sensing in aqueous solution (LOD = 3.82 ppb).[26] We also wished to compare the relative sensing abilities of these two polymers with that of polyethylene glycol (PEG), a polar, chemically robust polymer that is readily available in a variety of molecular weights. Through the evaluation of these three polymers, we hoped to establish whether these well-defined chemical reactions could provide a basis for detecting gas vapors with a WGM sensor.

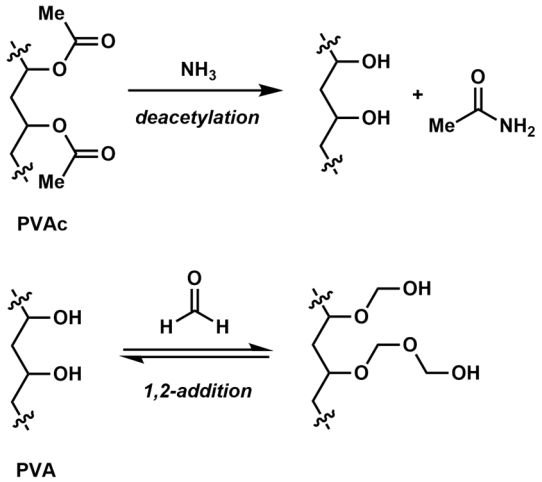

Figure 2. Chemical reactions proposed to enable the low concentration detection of gaseous ammonia and formaldehyde with polyvinyl acetate (PVAc) and polyvinyl alcohol (PVA) coatings on WGM gas sensors.

RESULTS AND DISCUSSION

Synthesis and deposition of polymer coatings

With consideration to literature precedent, we synthesized polymers with a (3-triethoxysilyl) propyl group to allow for efficient conjugation of an activated silica surface.[27] Samples of (3-triethoxysilyl) propyl-terminated polyethylene glycol (PEG) of two different molecular weights, 5000 Da and 20000 Da, were accessed by the chemical modification of commercially-available end-functionalized PEGs (Figure 3). Specifically, (3-triethoxysilyl) propyl-terminated PEG-5000 (siloxyPEG-5000) was accessed via a copper-catalyzed alkyne-azide cyclization from the corresponding alkyne-terminated PEG and (3-azidopropyl) triethoxysilane. 3-triethoxysilyl propyl-terminated PEG-20000 (siloxyPEG-20000) was synthesized by an amidation reaction between a succinimidyl ester-terminated PEG and (3-aminopropyl) triethoxysilane.

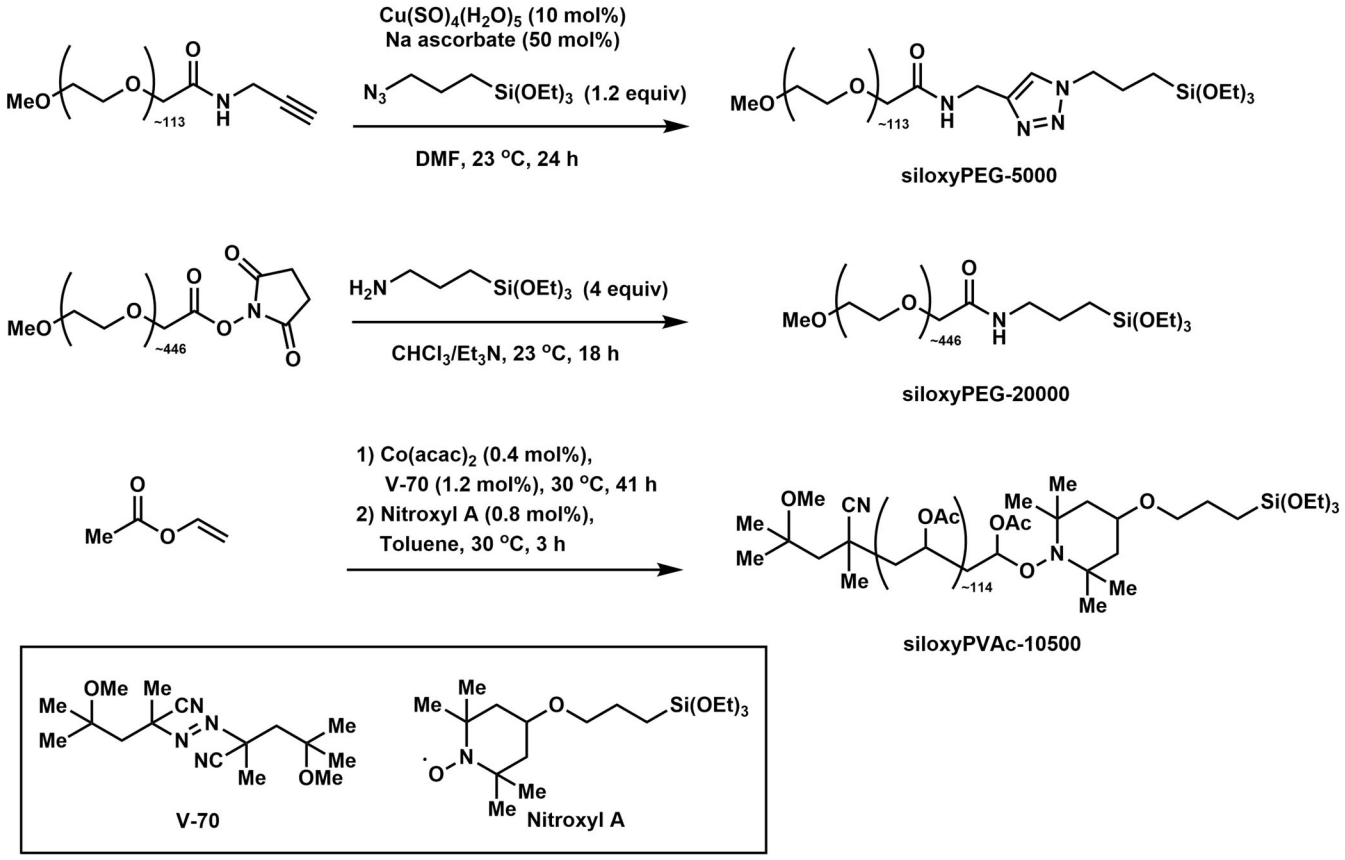

Figure 3. Synthetic routes to 3-(triethoxysilyl)propyl-terminated polyethylene glycols and polyvinyl acetate for direct grafting onto glass microtoroids.

In contrast, accessing (3-triethoxysilyl)propyl-terminated polyvinyl acetate (PVAc) required that the polymer be synthesized under living radical conditions, such that the desired end group could be installed in a well-defined manner. Vinyl acetate was successfully polymerized under cobalt-mediated conditions at 30°C using a combination of $Co(acac)_2$ (acac = acetylacetonate) and V-70 (2,2'-azobis(4-methoxy-2,4-dimethylvaleronitrile), a low temperature azo radical initiator). While these living polymerization conditions for vinyl acetate have been widely reported,[28,29] we implemented a less typical method for installing the desired end group: addition of a nitroxyl radical, a TEMPO derivative functionalized with a (3-triethoxysilyl)propyl group, lead to termination of the polymerization and allowed for the desired (3-triethoxysilyl)propyl-terminated PVAc (siloxyPVAc-10500) to be isolated. This nitroxide termination approach has been previously utilized to yield PVAc macroinitiators for ATRP.[29] Following purification of the polymer, NMR spectroscopy indicated that the desired end group has been installed with high efficiency (>95%). Furthermore, analytical gel permeation chromatography indicated a number average molecular weight (M_n) of approximately 10500 Da with a polydispersity (M_n/M_w) of 1.06. To our knowledge, there are no prior reports of a similar siloxy-terminated PVAc synthetized in a one-pot manner.

Siloxy-terminated polymers were deposited onto freshly prepared silica microtoroids by a solvothermal route. Generally, a 6 mM solution of the selected siloxy-terminated polymer in either chloroform or dimethyl sulfoxide (DMSO) was incubated with the bare microtoroid at room temperature for 2 hours. These conditions consistently yielded polymer-coated toroids with satisfactory optical properties, as characterized by a minimal decrease in quality factor (Q). A PVA-coated microtoroid was made by submerging a PVAc-coated microtoroid in a 3mM 200uL KOH/MeOH solution on a 45˚C hotplate for 1 hour. Following washing and the removal of residual solvent (dry N_2 stream or vacuum oven), the polymer-coated toroids were then evaluated in gas sensing experiments. Further synthesis details as well as nuclear magnetic resonance (NMR) spectra and size exclusion chromatography (SEC) data are provided in the Supplemental Information.

Sensitivity and selectivity tests of polymer-coated microtoroids

Gas sensing experiments were done in as controlled an environment as possible. The chamber is first initially filled with nitrogen. Air flow into the chamber is controlled by a flowmeter at 50 standard cubic centimeters per minute (sccm). Both wavelength shift and temperature change data are tracked and recorded simultaneously as the chamber fills with nitrogen. The thermal coefficient of the polymer-coated toroid is then determined and was found to be in the range of 2–8 pm/°C.[30,31] Subsequently, resonance frequency shifts were recorded in response to increases in concentration; all wavelength shift data is calibrated by previously obtained temperature

coefficients for each particular microtoroid (see Supplementary Information, Materials & Methods). Switching between the nitrogen carrier and the target gas was performed every ten minutes.

The response of toroids coated with PEG, PVAc and PVA coatings to DIMP, ammonia and formaldehyde at different concentrations are shown in Figures 4, 5, and 6 respectively. The gas concentrations range from 0.5 ppb to 4 ppb. PEG coated toroids show a much stronger reaction to DIMP than ammonia or formaldehyde (Figure 4), despite ammonia being readily dissolvable in liquid PEG at sub-atmospheric pressures,[32] and formaldehyde being a significant and persistent impurity in PEG owing to the decomposition of hydroxymethyl end groups in the polymer.[33] In our experiments, we believe the strongly polar phosphorous oxide bond in DIMP is responsible for its strong interactions with PEG as compared to those of ammonia or formaldehyde at the low concentrations employed in our gas sensing experiments. The presence of methoxy end groups, as opposed to hydroxyl end groups, in our PEG coatings suggests that the polymer is not being chemically modified by DIMP during our measurements. Experiments using a lower molecular weight PEG (5k) resulted in higher limits of detection (Supplementary Information).

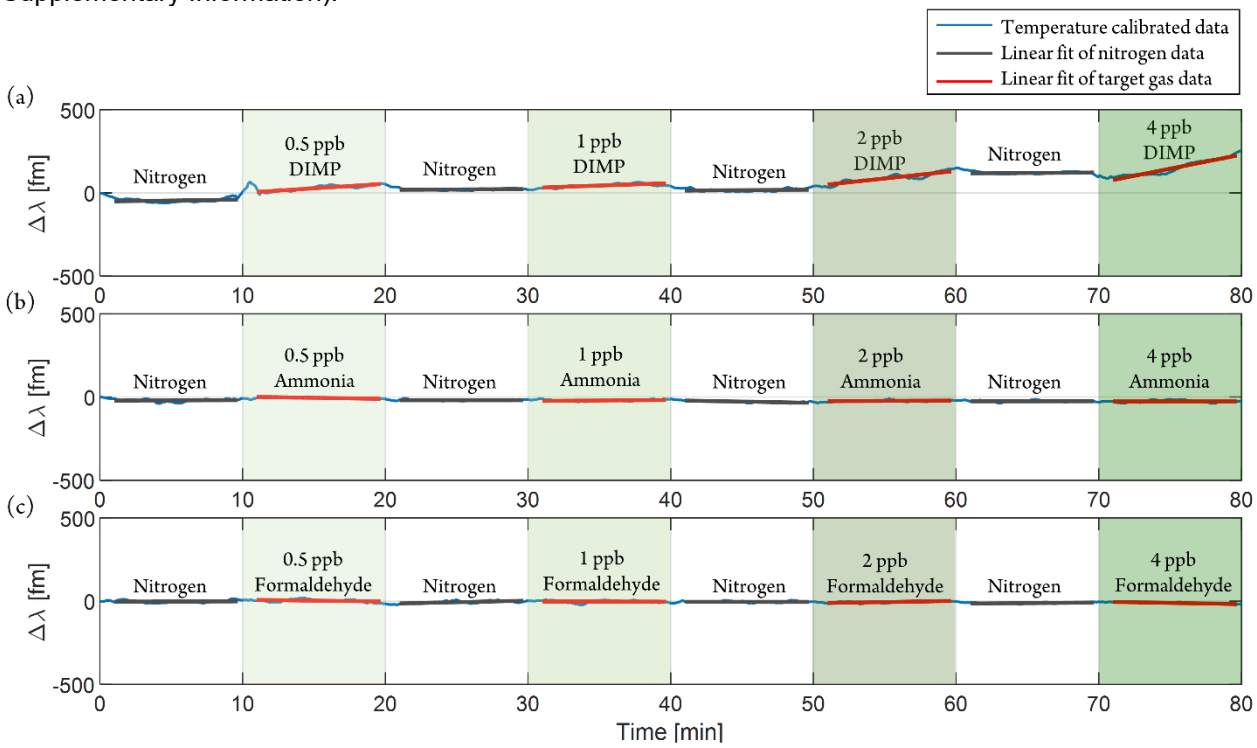

Figure 4. Response of a PEG-20k coated microtoroid to (a) DIMP, (b) ammonia, and (c) formaldehyde. PEG-20k-coated toroids show a shift to longer wavelengths in reaction with DIMP, but no discernible reaction to ammonia or formaldehyde.

Figure 5 indicates that the PVAc coating, similarly to PEG, has no strong interaction with formaldehyde that can provide a means of gas vapor detection with our WGM sensor. In contrast, PVAc displays strong sensitivity towards ammonia. For DIMP detection, the signal response is difficult to observe at low concentrations and is only apparent as the concentrations gradually increase to 2 ppb and higher, suggesting that the PVAc coating is much less sensitive to DIMP than the PEG coating was. In the detection of DIMP vapors by PVAc, the corresponding effective refractive index slightly decreases, resulting in a blue shift.

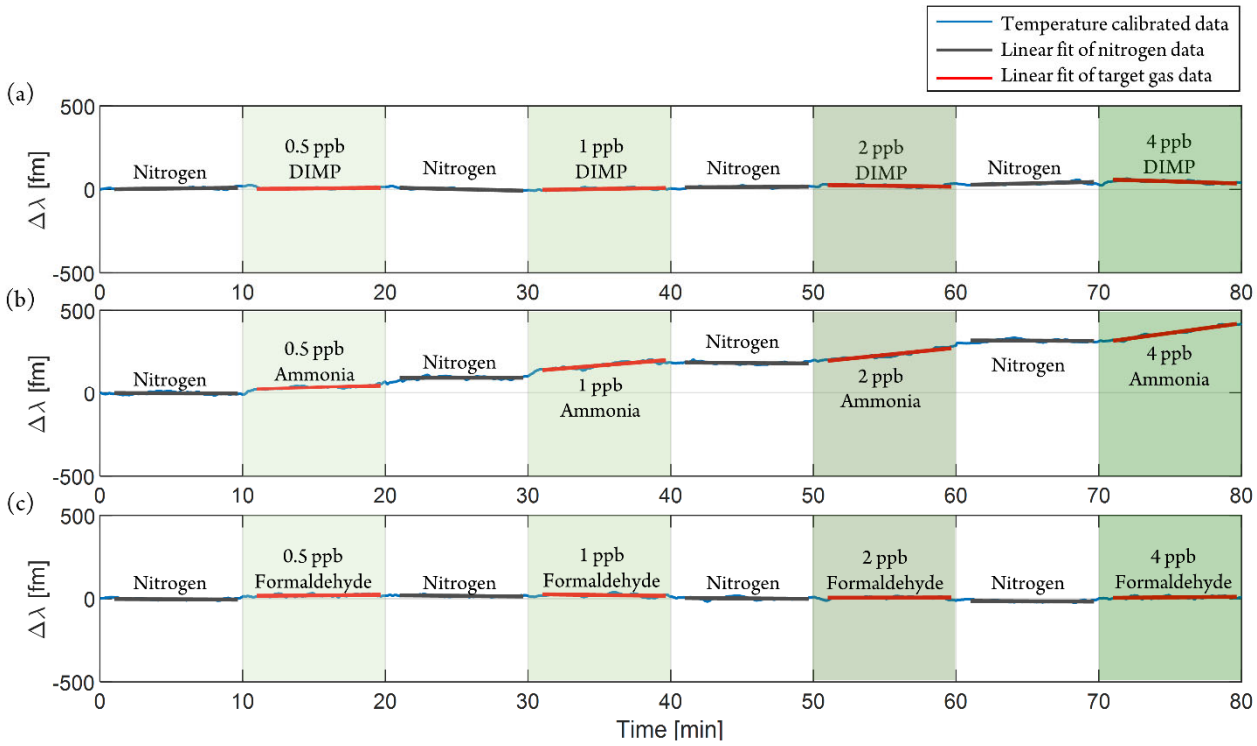

Figure 5. Response of a PVAc-10.5k coated microtoroid to (a) DIMP, (b) ammonia, and (c) formaldehyde. The PVAc-10.5k treated toroid shows a weak blue shift (shift to shorter wavelengths) in response to DIMP and a significant red shift in response to ammonia. Similar to PEG, PVAc-10.5k is non-reactive to formaldehyde.

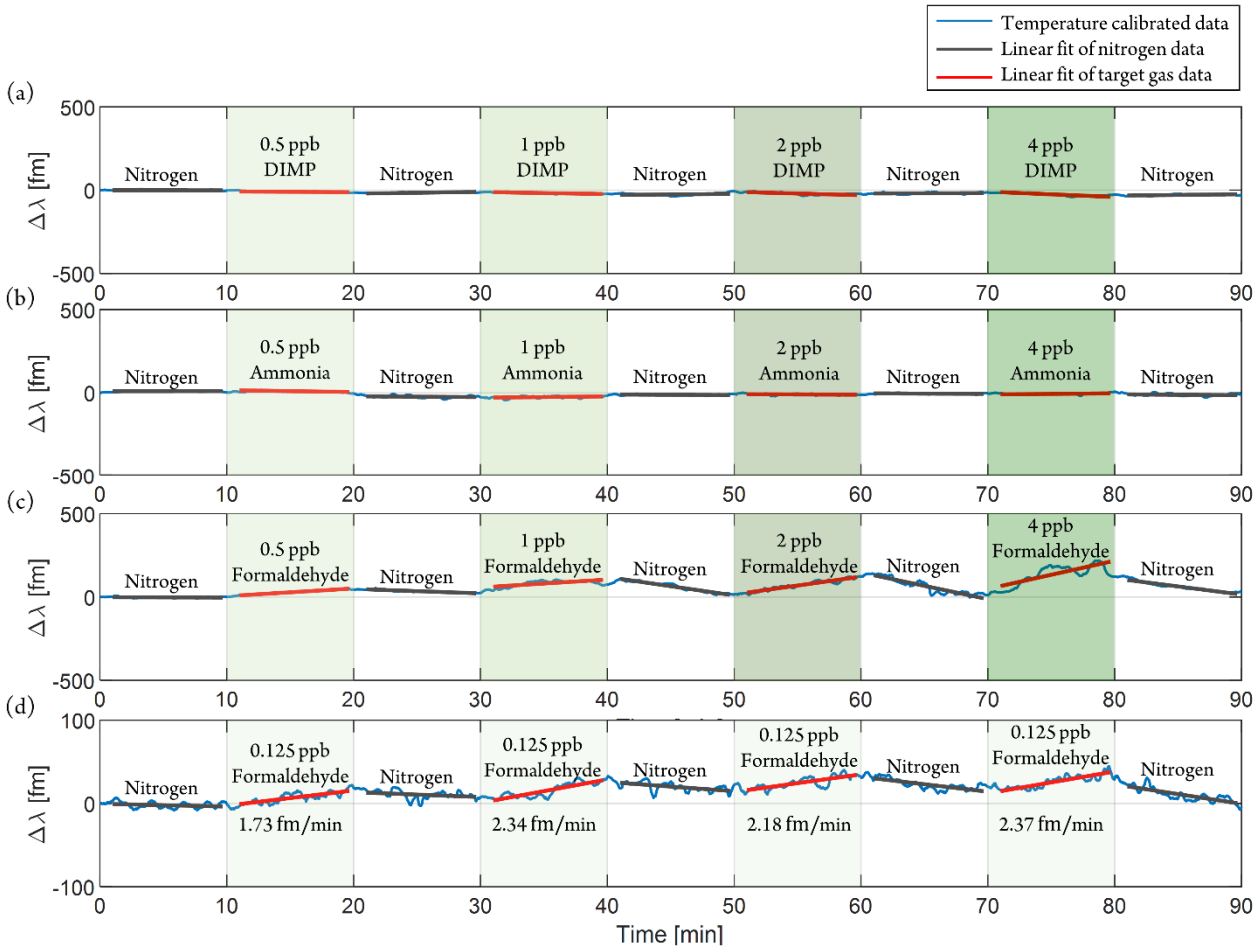

Figure 6. Response of a PVA coated microtoroid to (a) DIMP, (b) ammonia, and (c) formaldehyde. The PVA treated toroid presents a clear red shift (shift to longer wavelengths) in response to low concentrations of formaldehyde and a distinct reversible response after switching

back to pure nitrogen. The toroid sensors show a slight blue shift in response to DIMP and no response to ammonia. (d) Reproducibility of the sensor response at 125 ppt of formaldehyde.

The selectivity test of the PVA-treated toroid for the three gases is shown in Figure 6. It is apparent that the PVA no longer responds to ammonia after the alkaline hydrolysis of PVAc. PVA also has an extremely weak response to DIMP that results in a small blue shift of the sensor resonance frequency. These results provide some verification that the chemical reaction between ammonia and the acetate ester groups of PVAc underly its high sensitivity and selectivity for this analyte, as the lack of ester groups in PVA is correlated with no response to ammonia by the WGM sensor. The small response of PVA to DIMP may involve the exchange of isopropoxide bound to phosphorus for a polymer-based alkoxide; however, such alkoxide exchange reactions generally require elevated temperatures or microwave irradiation to proceed rapidly.[34] In contrast, the PVA-coated microtoroid WGM sensor displays extremely high sensitivity towards formaldehyde. After the removal of formaldehyde from the sample chamber, the signal recovered slowly to the initial position. The sensing and recovery experiment at 125 ppt of formaldehyde exposure (Figure 4d) shows excellent reversibility and reproducibility. While this analyte concentration is approaching the detection limit of the sensor (117 ppt, see below), it still responds quickly and consistently. These observations align with a reversible chemical process taking place, such as the 1,2-addition of alcohols to formaldehyde.

Figure of merit in FLOWER gas sensing

The sensitivity of the sensor is given in $\mathrm{fm\ min^{-1}\ ppb^{-1}}$. The background noise of the sensor can be calculated from three times the standard deviation (3σ) of the curve in response to nitrogen. The limit of detection (LOD) of FLOWER for different gases can be derived from the ratio of the background noise and sensitivity, written as[36]:

$$\mathrm{LOD\ [ppb]} = \frac{3\sigma_{\mathrm{Noise}}\ [\mathrm{fm \cdot min^{-1}}]}{\mathrm{Sensitivity\ [fm \cdot min^{-1} \cdot ppb^{-1}]}} \tag{3}$$

Figure 7a illustrates the procedure for calculating the sensitivity, background noise and LOD using the PVA coated toroid as an example. A greater sensitivity means that the absorption of a unit concentration of gas can cause a greater refractive index change or polymer swelling. A sensitivity heatmap of all the polymer-gas interactions tested is shown in Figure 7b. All three polymer coatings have excellent selectivity. Except for the reversible reaction of PVA with formaldehyde, all the nitrogen response sections are very flat. This enables sub ppb level detection limits at the (Table 1).

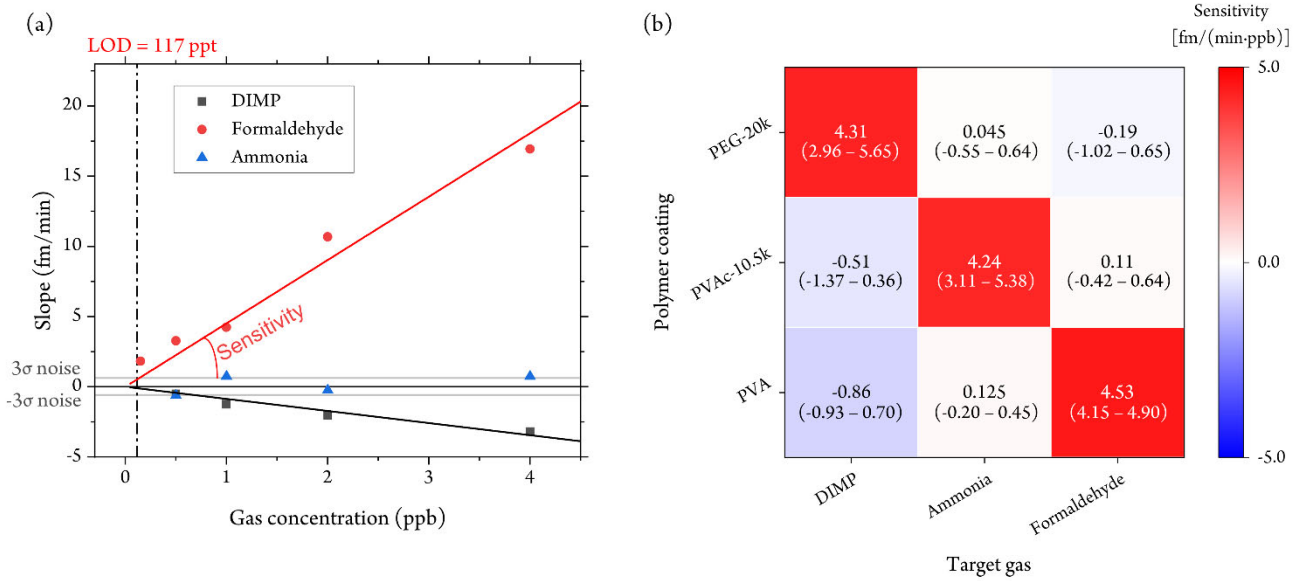

Figure 7. Sensitivity, selectivity, and limit of detection. (a) Sensing signal (slope of wavelength shift) of a PVA-coated toroid versus gas concentration. The sensitivity of the PVA coated toroid to the target gas is obtained by linearly fitting the points in the graph. The interaction of this line with the background noise is the detection limit. The LOD for formaldehyde sensing is 117 ppt. (b) Sensitivity heatmap of different coatings for different gases. The color represents the direction of wavelength shift (red for longer wavelength shifts and blue for shifts to shorter wavelengths). The intensity of the color shade indicates the interaction strength of the two chemicals. The 95% confidence intervals are given in parentheses.

Table 1. Summary of vapor sensing to DIMP, ammonia, formaldehyde.

Polymer	Gas	Background noise (3σ) [fm·min^{-1}]	Sensitivity [fm·min^{-1}·ppb^{-1}]	LOD [ppt]
PEG	DIMP	1.308	4.31	304
PVAc	Ammonia	1.842	4.86	379
PVA	Formaldehyde	0.532	4.53	117

Sensitivity and selectivity test of a mixed polymer coated microtoroid

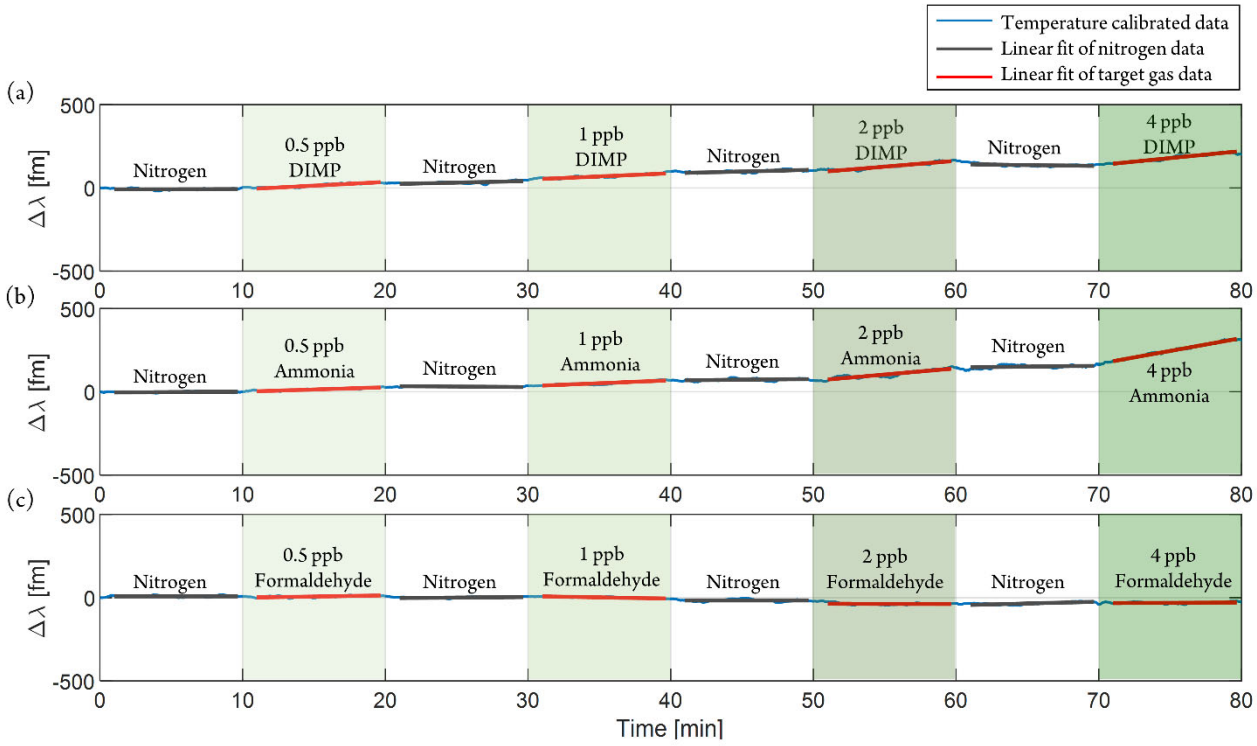

Figure 8. PEG and PVAc multilayer coated microtoroid response to (a) DIMP, (b) ammonia, and (c) formaldehyde. This multilayer coated toroid red shifts in response to both DIMP and ammonia but does not significantly respond to formaldehyde. The multilayer toroid's sensitivity to DIMP is slightly lower than to ammonia, which is influenced by the blueshift in response to PVAc and DIMP.

A mixture of polymers, PEG and PVAc, was used as a single coating on the toroid surface (Figure 8). Just as neither PEG nor PVAc were found to facilitate the detection of formaldehyde, the mixed coating of these polymers was also unresponsive to formaldehyde in our gas sensing tests. The mixed-coating toroid exhibited a noticeable redshift for ammonia, with a sensitivity of 3.83 fm min^{-1} ppb^{-1} that is well within the confidence interval shown in Figure 7b, and also showed a sensitivity of 3.45 fm min^{-1} ppb^{-1} for DIMP, appropriately combining the weak blue-shift effect of DIMP interacting with PVAc with the strong red shift associated with the interaction of DIMP with PEG. Overall, these experimental results are consistent with the sensitivity matrix in Figure 7b. These experiments suggest that FLOWER gas sensors may be modified to impart the sensor with sensitivity for specific analytes in a straightforward, combinatorial manner, overcoming one of the major limitations inherent to many gas sensing technologies.

Table 2. Comparison with other gas sensing technologies.

Gas	Sensing technique	LOD	Demonstrated LOD	Reference
DIMP	Present work	304 ppt	500 ppt	
	Paper spray mass spectrometry	A few ppb	A few ppb	[37]
	Organic polymerb Composite chemiresistive vapor detectors	6.6 ppb		[37]
Ammonia	Present work	379 ppt	500 ppt	
	Pristine graphene	33.2 ppt	200 ppt	[38]
	Pristine carbon nanotubes (CNTs)	27.8 ppt	200 ppt	[39]
	Silica gel coated microsphere	160 ppt	2.5 ppb	[39]
	SPR with metal oxide	154 ppb	10 ppm	[40]
	Graphene-enhanced Brillouin optomechanical microresonator	1 ppb	1 ppm	[42]
Formaldehyde	Present work	117 ppt	125 ppt	
	Carbon nanotubes	20 ppb	20 ppb	[42]
	SnO_2-nanowires	2 ppm	2 ppm	[43]

Table 2 provides a comparison of the WGM gas sensor in this paper with other gas sensing technologies for the detection of DIMP, ammonia, and formaldehyde. Using WGM gas sensors, we demonstrate lower detection limits than most gas sensing technologies and selective detection when combined with polymer layers. Graphene and CNTs have lower limits of detection based on extrapolation of sensitivity and noise levels, but similar minimum measured concentrations. Furthermore, these experiments using nanoscale carbon are performed in vacuum and lack selectivity.

Conclusion

We combine FLOWER with polymer coatings to create a highly selective as well as sensitive, small molecule gas sensor. We select three harmful gases as the targets for detection, namely DIMP, ammonia, and formaldehyde. By using three different polymer coatings, namely PEG, PVAc, and PVA, we demonstrate sub-ppb detection limits. The selectivity of the three individual coatings has also been verified to correspond to only one of the three analytes. With the reversible reaction of PVA with formaldehyde, the stability and reproducibility of the sensor at very low concentrations (125 ppt) have also been demonstrated. Furthermore, we realized selective and sensitive sensing by a mixed PEG/PVAc coating that performed in a combinatorial manner in comparison to the individual polymer coatings. This final set of experiments demonstrates applicability of these devices towards the selective detection of small molecule gas mixtures.

Acknowledgements

This project was funded by the Defense Threat Reduction Agency (HDTRA11810044).

References

(1) Liu, X.; Cheng, S.; Liu, H.; Hu, S.; Zhang, D.; Ning, H. A Survey on Gas Sensing Technology. *Sensors* **2012**, *12* (7), 9635–9665. https://doi.org/10.3390/s120709635.
(2) Nazemi, H.; Joseph, A.; Park, J.; Emadi, A. Advanced Micro- and Nano-Gas Sensor Technology: A Review. *Sensors* **2019**, *19* (6), 1285. https://doi.org/10.3390/s19061285.
(3) Kwak, D.; Lei, Y.; Maric, R. Ammonia Gas Sensors: A Comprehensive Review. *Talanta* **2019**, *204*, 713–730. https://doi.org/10.1016/j.talanta.2019.06.034.
(4) Yuan, Z.; Li, R.; Meng, F.; Zhang, J.; Zuo, K.; Han, E. Approaches to Enhancing Gas Sensing Properties: A Review. *Sensors* **2019**, *19* (7), 1495. https://doi.org/10.3390/s19071495.
(5) Han, T.; Nag, A.; Chandra Mukhopadhyay, S.; Xu, Y. Carbon Nanotubes and Its Gas-Sensing Applications: A Review. *Sensors and Actuators A: Physical* **2019**, *291*, 107–143. https://doi.org/10.1016/j.sna.2019.03.053.
(6) Chen, G.; Paronyan, T. M.; Pigos, E. M.; Harutyunyan, A. R. Enhanced Gas Sensing in Pristine Carbon Nanotubes under Continuous Ultraviolet Light Illumination. *Sci Rep* **2012**, *2* (1), 343. https://doi.org/10.1038/srep00343.
(7) Buckley, D. J.; Black, N. C. G.; Castanon, E. G.; Melios, C.; Hardman, M.; Kazakova, O. Frontiers of Graphene and 2D Material-Based Gas Sensors for Environmental Monitoring. *2D Mater.* **2020**, *7* (3), 032002. https://doi.org/10.1088/2053-1583/ab7bc5.
(8) Su, J.; Goldberg, A. F.; Stoltz, B. M. Label-Free Detection of Single Nanoparticles and Biological Molecules Using Microtoroid Optical Resonators. *Light: Science & Applications* **2016**, *5* (1), e16001. https://doi.org/10.1038/lsa.2016.1.
(9) Su, J. Label-Free Single Exosome Detection Using Frequency-Locked Microtoroid Optical Resonators. *ACS Photonics* **2015**, *2* (9), 1241–1245. https://doi.org/10.1021/acsphotonics.5b00142.
(10) Li, C.; Chen, L.; McLeod, E.; Su, J. Dark Mode Plasmonic Optical Microcavity Biochemical Sensor. *Photon. Res.* **2019**, *7* (8), 939. https://doi.org/10.1364/PRJ.7.000939.
(11) Su, J. Label-Free Biological and Chemical Sensing Using Whispering Gallery Mode Optical Resonators: Past, Present, and Future. *Sensors* **2017**, *17* (3), 540. https://doi.org/10.3390/s17030540.
(12) Chen, L.; Li, C.; Liu, Y.-M.; Su, J.; McLeod, E. Simulating Robust Far-Field Coupling to Traveling Waves in Large Three-Dimensional Nanostructured High-Q Microresonators. *Photon. Res.* **2019**, *7* (9), 967. https://doi.org/10.1364/PRJ.7.000967.
(13) Chen, L.; Li, C.; Liu, Y.; Su, J.; McLeod, E. Three-Dimensional Simulation of Particle-Induced Mode Splitting in Large Toroidal Microresonators. *Sensors* **2020**, *20* (18), 5420. https://doi.org/10.3390/s20185420.
(14) Jiang, X.; Qavi, A. J.; Huang, S. H.; Yang, L. Whispering Gallery Microsensors: A Review. *Matter* **2020**, *3* (2), 371–392. https://doi.org/10.1016/j.matt.2020.07.008.
(15) Sun, Y.; Fan, X. Analysis of Ring Resonators for Chemical Vapor Sensor Development. *Opt. Express* **2008**, *16* (14), 10254. https://doi.org/10.1364/OE.16.010254.
(16) Luchansky, M. S.; Bailey, R. C. High- *Q* Optical Sensors for Chemical and Biological Analysis. *Anal. Chem.* **2012**, *84* (2), 793–821. https://doi.org/10.1021/ac2029024.
(17) Arnold, S.; Khoshsima, M.; Teraoka, I.; Holler, S.; Vollmer, F. Shift of Whispering-Gallery Modes in Microspheres by Protein Adsorption. *Optics Letters* **2003**, *28* (4), 272. https://doi.org/10.1364/OL.28.000272.

(18) Passaro, V. M. N.; Dell'Olio, F.; De Leonardis, F. Ammonia Optical Sensing by Microring Resonators. *Sensors* **2007**, *7* (11), 2741–2749. https://doi.org/10.3390/s7112741.
(19) Righini, G. C.; Berneschi, S.; Cosci, A.; Farnesi, D.; Giannetti, A.; Conti, G. N.; Pelli, S.; Soria, S. Advanced Sensing by WGM Microresonators. In *Advanced Photonics 2017 (IPR, NOMA, Sensors, Networks, SPPCom, PS)*; OSA: New Orleans, Louisiana, 2017; p SeM2E.5. https://doi.org/10.1364/SENSORS.2017.SeM2E.5.
(20) Lemieux-Leduc, C.; Guertin, R.; Bianki, M.-A.; Peter, Y.-A. All-Polymer Whispering Gallery Mode Resonators for Gas Sensing. *Opt. Express* **2021**, *29* (6), 8685. https://doi.org/10.1364/OE.417703.
(21) Fiandor, J.; García-López, M. T.; Heras, F. G. D. L.; Méndez-Castrillón, P. P. A Facile Regioselective 1-O-Deacylation of Peracylated Glycopyranoses. *Synthesis* **1985**, *1985* (12), 1121–1123. https://doi.org/10.1055/s-1985-31446.
(22) Wang, H.; Xu, R.; Liang, S.; Ran, F.; Zhang, L.; Zhang, Y.; Zhou, D.; Xiao, S. Selective and Facile Deacetylation of Pentacyclic Triterpenoid under Methanolic Ammonia Condition and Unambiguous NMR Analysis. *Chinese Chemical Letters* **2020**, *31* (2), 333–336. https://doi.org/10.1016/j.cclet.2019.06.007.
(23) Gaca, K. Z.; Parkinson, J. A.; Lue, L.; Sefcik, J. Equilibrium Speciation in Moderately Concentrated Formaldehyde–Methanol–Water Solutions Investigated Using ^{13}C and ^{1}H Nuclear Magnetic Resonance Spectroscopy. *Ind. Eng. Chem. Res.* **2014**, *53* (22), 9262–9271. https://doi.org/10.1021/ie403252x.
(24) Barakoti, K. K.; Subedi, P.; Chalyavi, F.; Gutierrez-Portocarrero, S.; Tucker, M. J.; Alpuche-Aviles, M. A. Formaldehyde Analysis in Non-Aqueous Methanol Solutions by Infrared Spectroscopy and Electrospray Ionization. *Frontiers in Chemistry* **2021**, *9*.
(25) Roto, R.; Rianjanu, A.; Fatyadi, I. A.; Kusumaatmaja, A.; Triyana, K. Enhanced Sensitivity and Selectivity of Ammonia Sensing by QCM Modified with Boric Acid-Doped PVAc Nanofiber. *Sensors and Actuators A: Physical* **2020**, *304*, 111902. https://doi.org/10.1016/j.sna.2020.111902.
(26) Aksornneam, L.; Kanatharana, P.; Thavarungkul, P.; Thammakhet, C. 5-Aminofluorescein Doped Polyvinyl Alcohol Film for the Detection of Formaldehyde in Vegetables and Seafood. *Anal. Methods* **2016**, *8* (6), 1249–1256. https://doi.org/10.1039/C5AY02719E.
(27) Glosz, K.; Stolarczyk, A.; Jarosz, T. Siloxanes—Versatile Materials for Surface Functionalisation and Graft Copolymers. *International Journal of Molecular Sciences* **2020**, *21* (17), 6387. https://doi.org/10.3390/ijms21176387.
(28) Debuigne, A.; Caille, J.-R.; Detrembleur, C.; Jérôme, R. Effective Cobalt Mediation of the Radical Polymerization of Vinyl Acetate in Suspension. *Angewandte Chemie International Edition* **2005**, *44* (22), 3439–3442. https://doi.org/10.1002/anie.200500112.
(29) Debuigne, A.; Caille, J.-R.; Willet, N.; Jérôme, R. Synthesis of Poly(Vinyl Acetate) and Poly(Vinyl Alcohol) Containing Block Copolymers by Combination of Cobalt-Mediated Radical Polymerization and ATRP. *Macromolecules* **2005**, *38* (23), 9488–9496. https://doi.org/10.1021/ma051246x.
(30) Vollmer, F.; Yang, L. Review Label-Free Detection with High-Q Microcavities: A Review of Biosensing Mechanisms for Integrated Devices. *Nanophotonics* **2012**, *1* (3–4), 267–291. https://doi.org/10.1515/nanoph-2012-0021.
(31) Ozgur, E.; Roberts, K. E.; Ozgur, E. O.; Gin, A. N.; Bankhead, J. R.; Wang, Z.; Su, J. Ultrasensitive Detection of Human Chorionic Gonadotropin Using Frequency Locked Microtoroid Optical Resonators. *Anal. Chem.* **2019**, *91* (18), 11872–11878. https://doi.org/10.1021/acs.analchem.9b02630.
(32) Zhang, J.-B.; Huang, K. Solubilities of Ammonia in Polyethylene Glycols at 298.2–353.2 K and 0–200 KPa. *J. Chem. Eng. Data* **2020**, *65* (1), 97–105. https://doi.org/10.1021/acs.jced.9b00779.
(33) Hildebrandt, C.; Joos, L.; Saedler, R.; Winter, G. The "New Polyethylene Glycol Dilemma": Polyethylene Glycol Impurities and Their Paradox Role in MAb Crystallization. *Journal of Pharmaceutical Sciences* **2015**, *104* (6), 1938–1945. https://doi.org/10.1002/jps.24424.
(34) Bálint, E.; Tajti, Á.; Tóth, N.; Keglevich, G. Continuous Flow Alcoholysis of Dialkyl H-Phosphonates with Aliphatic Alcohols. *Molecules* **2018**, *23* (7), 1618. https://doi.org/10.3390/molecules23071618.
(35) MacDougall, Daniel.; Crummett, W. B.; et al., . Guidelines for Data Acquisition and Data Quality Evaluation in Environmental Chemistry. *Anal. Chem.* **1980**, *52* (14), 2242–2249. https://doi.org/10.1021/ac50064a004.
(36) McKenna, J.; S. Dhummakupt, E.; Connell, T.; S. Demond, P.; B. Miller, D.; Nilles, J. M.; E. Manicke, N.; Glaros, T. Detection of Chemical Warfare Agent Simulants and Hydrolysis Products in Biological Samples by Paper Spray Mass Spectrometry. *Analyst* **2017**, *142* (9), 1442–1451. https://doi.org/10.1039/C7AN00144D.
(37) Hopkins, A. R.; Lewis, N. S. Detection and Classification Characteristics of Arrays of Carbon Black/Organic Polymer Composite Chemiresistive Vapor Detectors for the Nerve Agent Simulants Dimethylmethylphosphonate and Diisopropylmethylphosponate. *Anal. Chem.* **2001**, *73* (5), 884–892. https://doi.org/10.1021/ac0008439.
(38) Chen, G.; Paronyan, T. M.; Harutyunyan, A. R. Sub-Ppt Gas Detection with Pristine Graphene. *Appl. Phys. Lett.* **2012**, *101* (5), 053119. https://doi.org/10.1063/1.4742327.

(39) Mallik, A. K.; Farrell, G.; Liu, D.; Kavungal, V.; Wu, Q.; Semenova, Y. Silica Gel Coated Spherical Micro Resonator for Ultra-High Sensitivity Detection of Ammonia Gas Concentration in Air. *Sci Rep* **2018**, *8* (1), 1620. https://doi.org/10.1038/s41598-018-20025-9.
(40) Pathak, A.; Mishra, S. K.; Gupta, B. D. Fiber-Optic Ammonia Sensor Using Ag/SnO_2 Thin Films: Optimization of Thickness of SnO_2 Film Using Electric Field Distribution and Reaction Factor. *Appl. Opt., AO* **2015**, *54* (29), 8712–8721. https://doi.org/10.1364/AO.54.008712.
(41) Yao, B.; Yu, C.; Wu, Y.; Huang, S.-W.; Wu, H.; Gong, Y.; Chen, Y.; Li, Y.; Wong, C. W.; Fan, X.; Rao, Y. Graphene-Enhanced Brillouin Optomechanical Microresonator for Ultrasensitive Gas Detection. *Nano Lett.* **2017**, *17* (8), 4996–5002. https://doi.org/10.1021/acs.nanolett.7b02176.
(42) Xie, H.; Sheng, C.; Chen, X.; Wang, X.; Li, Z.; Zhou, J. Multi-Wall Carbon Nanotube Gas Sensors Modified with Amino-Group to Detect Low Concentration of Formaldehyde. *Sensors and Actuators B: Chemical* **2012**, *168*, 34–38. https://doi.org/10.1016/j.snb.2011.12.112.
(43) Castro-Hurtado, I.; Herrán, J.; Ga Mandayo, G.; Castaño, E. SnO2-Nanowires Grown by Catalytic Oxidation of Tin Sputtered Thin Films for Formaldehyde Detection. *Thin Solid Films* **2012**, *520* (14), 4792–4796. https://doi.org/10.1016/j.tsf.2011.10.140.